

## Supplementary tables

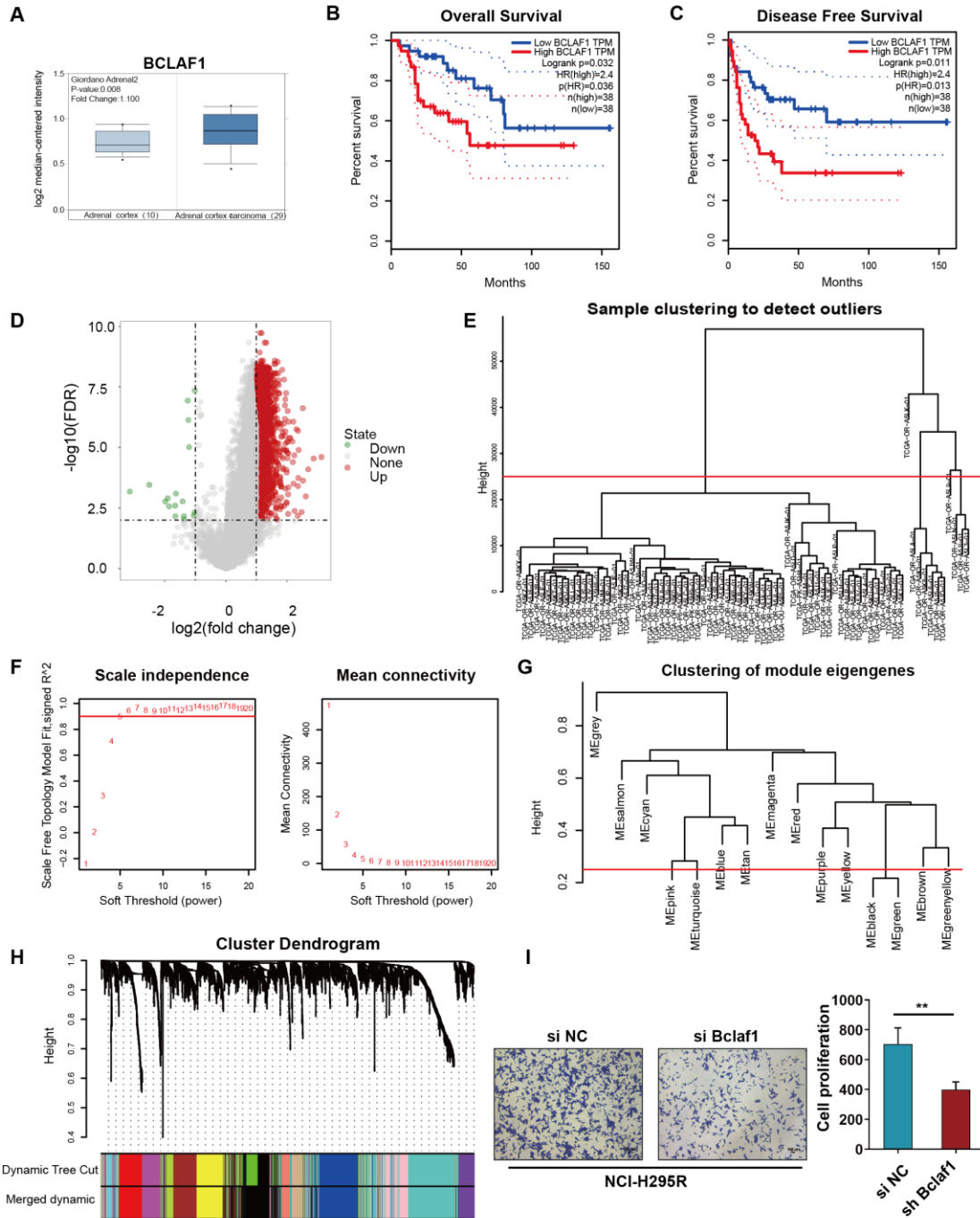
**Table S1. Sequence of siRNAs or qPCR primers used in this study.**

Name	Sequence (5'-3')	
	Forward (5'-3')	Reverse (5'-3')
BCLAF1 -siRNA	GCAGAGGGCGCUUUAACUUTT	AAGUUAAGCGCCCUCUGCTT
CDK1 (human)	GGAAGGGGTTCTAGTACTGC	TGGAATCCTGCATAAGCACA
CCNB1 (human)	ACCAAATACCTACTGGGTCGG	GCATGAACCGATCAATAATGG
$\beta$ -actin (human)	CACCACACCTTCTACAATGAGCTGC	ACAGCCTGGATAGCAACGTACATGG

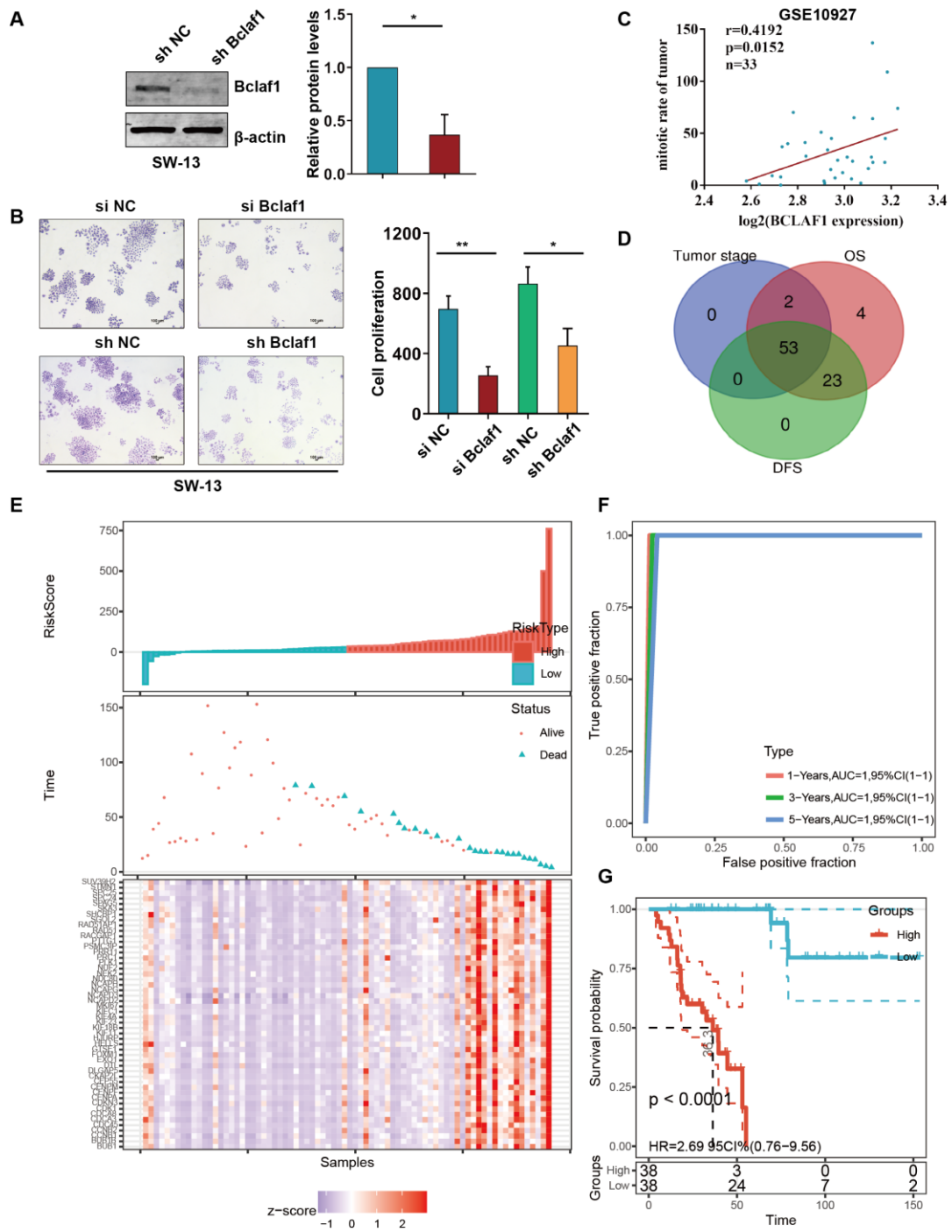
**Table S2. Antibodies used in this study.**

Name	Species	Manufacturer	Product Code	Application in this study
Bclaf1	human	Proteintech	26809-1-AP	WB
CDK1	human	Abcam	ab133327	WB, IHC
Cyclin B1	human	Abcam	ab32053	WB, IHC
$\beta$ -actin	human	Ray biotech	antibody RM2001	WB

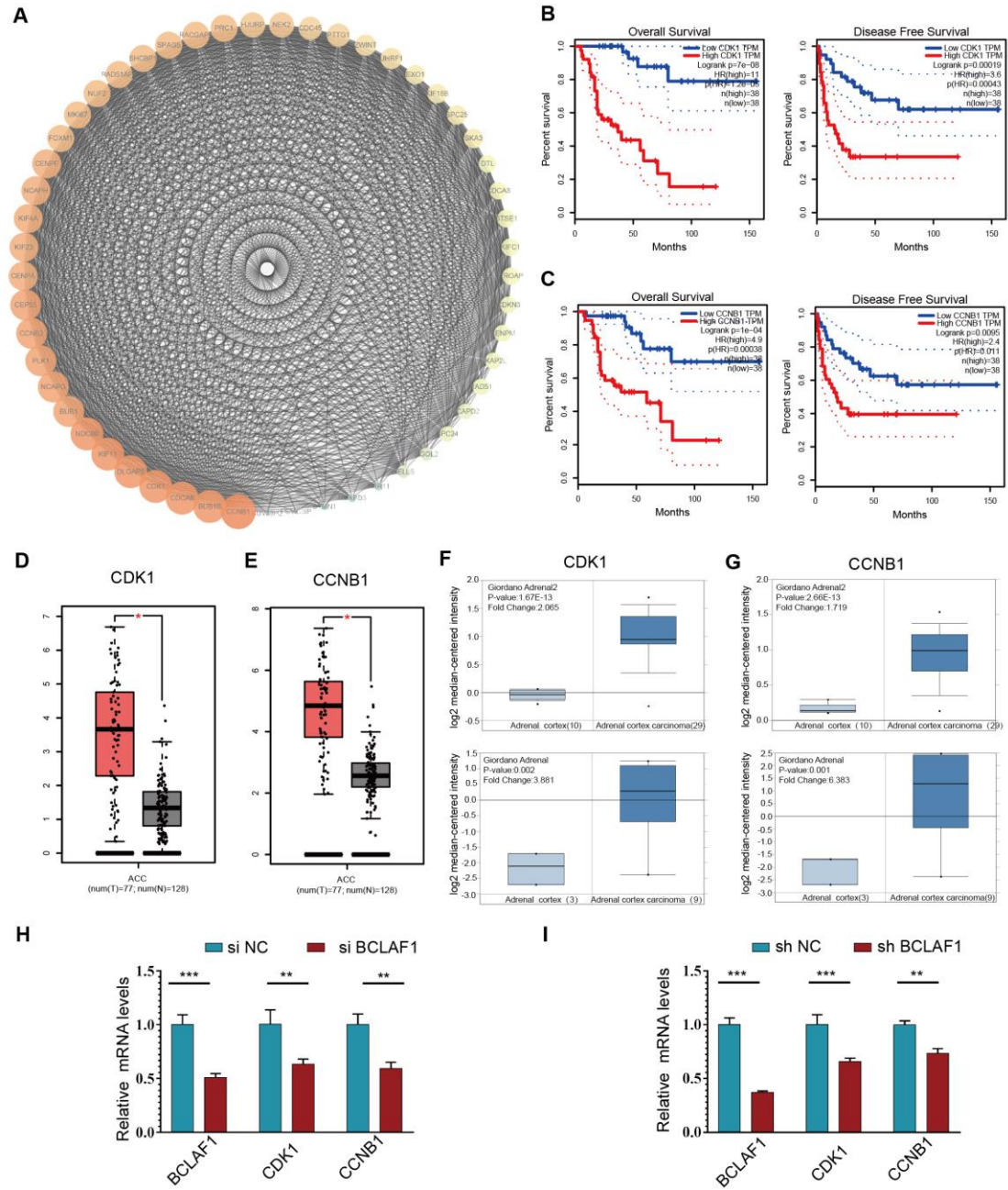
# Supplementary figure



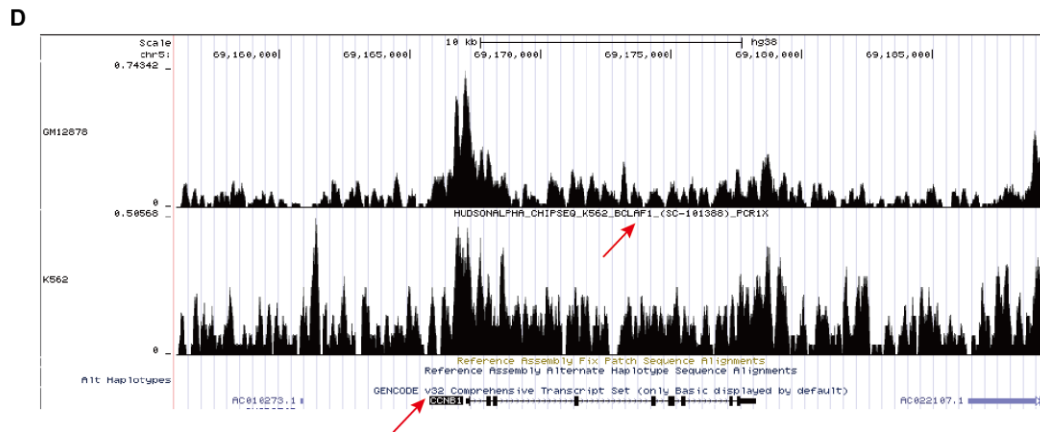
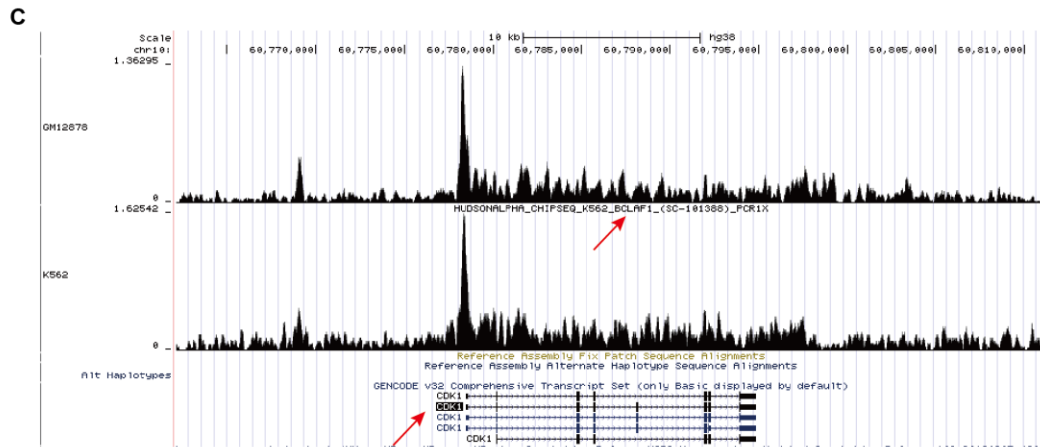
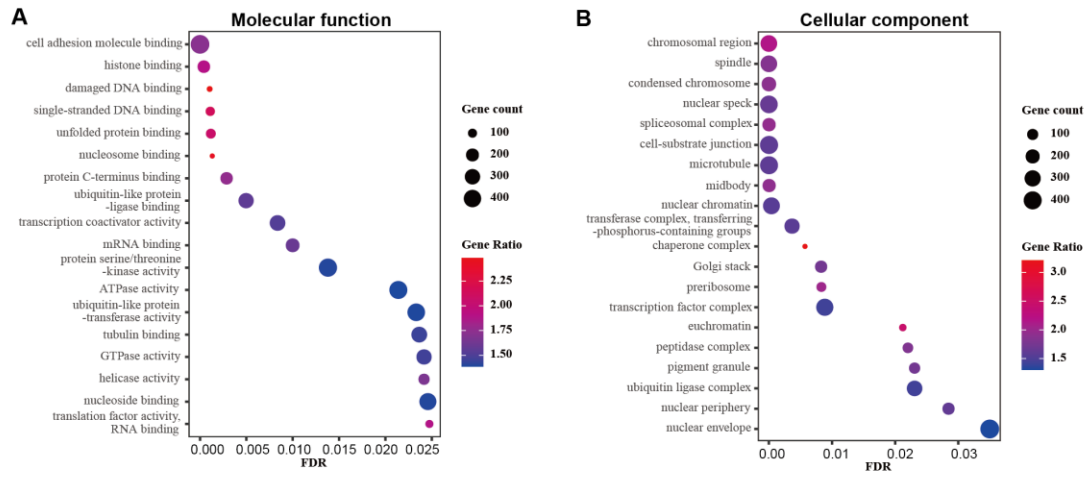
[316599]Figure S[1]



[316599]Figure S[2]



[316599]Figure S[3]



[316599]Figure S[4]

## Supplementary figure legends

**Figure S1.** A Differential analysis between adrenal cortex carcinoma and normal adrenal cortex performed through an analysis of the Oncomine database. B, C Kaplan-Meier plots showing OS rates (B) and DFS rates (C) for the high-BCLAF1 and low-BCLAF1 groups. P values were calculated using the log-rank test. D Volcano plots were created to illustrate the distribution of DEGs. The vertical line indicates  $|\log_2FC| = 1$ . E Clustering of 76 samples after excluding outliers (height > 25000). F Determination of the soft thresholding power ( $\beta=6$ ) for gene clustering. G Merging of clustered modules with height < 0.25. H Hierarchical clustering dendrograms of identified coexpressed genes in 14 modules. I The cell proliferation was determined after crystal violet staining by wide field microscopy.

**Figure S2.** A Bclaf1 was downregulated by stably integrated BCLAF1-shRNA expression construct. B The cell proliferation was determined by crystal violet staining after knockdown of Bclaf1. C Correlation between Bclaf1 expression and the tumour mitotic rate. D Venn diagram presenting the overlap between different types of clinical information. E Relationship between gene expression and patient survival status. The patients were graded into high-risk and low-risk groups based on their survival status and gene expression (upper panel). The patients' follow-up times are plotted in the middle panel, and the blue triangle indicates death. The expression of 53 genes is illustrated by the heatmap (lower panel). F ROC curve constructed to evaluate the survival status based on the risk score. Coloured curves described the ability to predict the outcome of the patient's death at 1, 3, and 5 years of follow-up. G Survival analysis of patients in the high-risk vs. low-risk groups.

**Figure S3.** A PPI network of 53 genes. The larger, darker nodes represent higher-degree

nodes. B, C Kaplan-Meier plots showing OS rates and DFS rates for the two core genes. D, E Box plots of (D) CDK1 and (E) CCNB1 based on the TCGA database and matched GTEx normal-tissue database. F, G Differential analysis between adrenal cortex carcinoma and normal adrenal cortex performed by OncoPrint database analysis. H, I Downregulation of CDK1 and CCNB1 via BCLAF1 knockdown after cell transfection. The mRNA levels were assessed by RT-qPCR.  $**p < 0.01$ , and  $***p < 0.001$  vs. the control.

**Figure S4.** A, B Plot of the GO enrichment analysis. The molecular function (MF) and cellular component (CC) terms are illustrated. C, D ChIP-seq performed with the Cistrome Data Browser: a peak near a transcription start site (TSS) indicates that Bclaf1 has a binding signal at this locus.